The debris disk candidates: eleven 24 μm excess stars in the *Spitzer* SWIRE fields

2012 Res. Astron. Astrophys. 12 513

(http://iopscience.iop.org/1674-4527/12/5/004)

Research in Astron. Astrophys. **2012** Vol. **12** No. **5**, 513–528
http://www.raa-journal.org *http://www.iop.org/journals/raa*

Research in Astronomy and Astrophysics

The debris disk candidates: eleven 24 μm excess stars in the *Spitzer* SWIRE fields *

Hong Wu[1], Chao-Jian Wu[2], Chen Cao[3,4], Sebastian Wolf[5] and Jing-Yao Hu[1]

[1] Key Laboratory of Optical Astronomy, National Astronomical Observatories, Chinese Academy of Sciences, Beijing 100012, China; *hwu@bao.ac.cn*
[2] Department of Astronomy, Beijing Normal University, Beijing 100875, China
[3] Institute of Space Science and Physics, Shandong University at Weihai, Weihai 264209, China
[4] Shandong Provincial Key Laboratory of Optical Astronomy & Solar-Terrestrial Environment, Weihai 264209, China
[5] Max Planck Institute for Astronomy, Königstuhl 17, 69117 Heidelberg, Germany

Received 2011 September 27; accepted 2012 February 4

Abstract We present the optical to mid-infrared SEDs of 11 debris disk candidates from *Spitzer* SWIRE fields. All the candidates are selected from SWIRE 24 μm sources matched with both the SDSS star catalog and the 2MASS point source catalog. They show an excess in the mid-infrared at 24 μm (K_S–$[24]_{\rm Vega} \geq 0.44$), indicating the presence of a circumstellar dust disk. The observed optical spectra show that they are all late-type main-sequence stars covering the spectral types of FGKM. Their fractional luminosities are well above 5×10^{-5}, even up to the high fractional luminosity of 1×10^{-3}. The high galactic latitudes of SWIRE fields indicate that most of these candidates could belong to the oldest stars in the thick disk. Our results indicate that high fractional luminosity debris disks could exist in old solar-like star systems, though they are still quite rare. Their discovery at high galactic latitudes also provides an excellent opportunity for further study of the properties and evolution of debris disks in regions of the Galaxy with low densities of ISM, called ISM poor environments.

Key words: infrared: stars — planetary systems: protoplanetary disks — stars: formation

1 INTRODUCTION

One of the most notable achievements of the *InfraRed Astronomical Satellite* (IRAS) is the discovery of dusty circumstellar disks (Zuckerman 2001). An example of this is Vega, which shows a large infrared excess from a main-sequence star (Aumann et al. 1984). This provided the first direct evidence for the existence of a debris disk. The scattered light from several nearby debris disks has been analyzed by the HST (Krist et al. 2005). Debris disks are thought to be formed from dissipated, optically thick accretion disks left over from star formation (Hollenbach et al. 2000; Wyatt & Dent 2002;

* Supported by the National Natural Science Foundation of China.

Gorlova et al. 2004). The study of debris disks is crucial to understanding the formation and existence of planets (Bryden et al. 2009) and smaller objects, such as comets and asteroids (Zuckerman 2001).

Limited by the sensitivity of IRAS, most of the debris disks that have been discovered were from nearby stars much younger than the Sun (Metchev et al. 2004; Bryden et al. 2006) since they are likely to be at a transition stage with a higher probability of possessing disks with plenty of dust (Zuckerman & Song 2004; Bryden et al. 2006), and their luminosities are high enough to heat a debris disk to a level detectable by IRAS (Krist et al. 2005). With higher sensitivity, better resolution and a more extended wavelength range (Jourdain de Muizon et al. 1999), the *Infrared Space Observatory (ISO)* has expanded our capability to search for circumstellar dust (Spangler et al. 2001) to the modest infrared excess among older stars (Decin et al. 2000, 2003; Habing et al. 2001).

With the launch of the *Spitzer* Space Telescope (Werner et al. 2004), a new level of sensitivity and spatial resolution is available for studies of debris disks in the infrared (Su et al. 2005). It provides the potential to identify and investigate debris systems that were not detectable with previous observatories (Kim et al. 2005), and extends the search for debris disks to larger distances (Bryden et al. 2006). Several *Spitzer* programs have focused on this field, including the Cores to Disks (Evans et al. 2003, C2D), the Formation and Evolution of Planetary Systems (Meyer et al. 2004, FEPS), the Galactic Legacy Infrared Mid-plane Survey Extraordinaire (Benjamin et al. 2003, GLIMPSE) and the Survey of Solar-Type Stars (Beichman et al. 2005, SSS). However, most of these programs are designed to search for the infrared excess in either known nearby planetary systems or debris systems in regions where interstellar material is rich, such as low galactic latitude regions and molecular clouds. At high galactic latitudes, there are also some wide-area surveys from the Multiband Imaging Photometer for *Spitzer* (Rieke et al. 2004, MIPS), such as the NOAO Deep Wide-Field Survey (Jannuzi & Dey 1999; Houck et al. 2005; Brand et al. 2006), the *Spitzer* Wide-Area Infrared Extragalactic Survey (Lonsdale et al. 2003, SWIRE) and the *Spitzer* Extragalactic First Look Survey (Fadda et al. 2006, xFLS), which provide us with more star candidates showing infrared excesses (Hovhannisyan et al. 2009).

The *Spitzer* SWIRE campaign was observed in the four mid-infrared IRAC bands (3.6, 4.5, 5.8, 8.0 μm) (Fazio et al. 2004) and the three mid-to-far infrared MIPS bands (24, 70, 160 μm) (Rieke et al. 2004). Designed for extragalactic surveys, all six SWIRE fields are at high galactic latitudes and cover about 50 deg^2. The wide field and high sensitivity provide us an opportunity to search for new faint debris disk candidates, and even planets (Bryden et al. 2009) in the thick disk or halo. Contrary to the other *Spitzer* programs mentioned above, which focus on younger or nearby systems, the debris disk candidates selected from SWIRE fields are much farther in distance, from 300 to 2000 pc compared with 10 to 150 pc in FEPS, and much older, with the oldest systems being about 10 Gyr. Generally, a star that is older than 10 Myr can be regarded as a debris disk candidate (Gorlova et al. 2006). This sample will help us to explore the formation of planetary systems in regions of the Galaxy with low densities of ISM, called ISM poor environments.

In this paper, we first describe the optical to infrared observations, data reduction and candidate selection in Section 2. In Section 3 we give the infrared properties of the stars showing excess in 24 μm and their spectral energy distributions (SEDs). The discussion and summary are respectively presented in Sections 4 and 5.

2 DATA, OBSERVATIONS AND CANDIDATE SELECTION

2.1 *Spitzer* Mid-Infrared Data and Data Reductions

The 24 μm excess stars are from the ELAIS-N1, ELAIS-N2 and Lockman Hole fields of the SWIRE fields. The overlapping regions of observation between IRAC and MIPS for the ELAIS-N1, ELAIS-N2 and Lockman Hole fields are about 8, 4 and 11 deg^2 respectively. The BCD (basic calibrated

data) images of the four IRAC bands were obtained from *Spitzer* Science Center, and include flat-field corrections, dark subtractions, and linearity and flux calibrations (Fazio et al. 2004). The IRAC images were mosaiced from the BCD images after pointing refinement, distortion correction and cosmic-ray removal with a final pixel scale of $0.6''$, as described by Huang et al. (2004) and Wu et al. (2005), while the MIPS 24 μm images were mosaiced in a similar way with a final pixel scale of $1.225''$(Wen et al. 2007; Cao & Wu 2007). Matching the sources detected by the SExtractor (Bertin & Arnouts 1996) in the five bands (the four IRAC bands and the MIPS 24 μm band) with the 2MASS sources, we obtained astrometric uncertainties of less than $0.5''$.

The mid-infrared photometries were obtained by the SExtractor, with an aperture of $3''$ for the four IRAC bands and $10.0''$ for the MIPS 24 μm band. All these magnitudes are in the AB magnitude system (Oke & Gunn 1983) and all the magnitudes of the four IRAC bands were corrected for the aperture of $24''$. Comparing with the model colors of the IRAC magnitudes and the 2MASS K_S magnitude (Cutri et al. 2003) for the 2MASS stars with J–$K_S \leq 0.3$, as Lacy et al. (2005) did for the sources in the *Spitzer* xFLS field, small additional corrections were made for all four IRAC bands. These give us calibration errors in the four IRAC bands of better than 0.08 mag. As for 24 μm, the magnitudes were corrected to an aperture of $30''$. The calibration accuracy of 24 μm is better than 10% (Rieke et al. 2004). The 5σ flux in the four IRAC bands and the MIPS 24 μm band are about 5, 8, 43, 43 and 200 μJy, respectively.

2.2 Optical and Near-IR Photometries

The ELAIS-N1, Lockman Hole and ELAIS-N2 fields are completely or partly covered by the Sloan Digital Sky Survey (Stoughton et al. 2002, SDSS) and the total overlap regions used in this work are about 15 deg^2. All the *Spitzer* sources were matched with the SDSS point sources from the "Star" catalog of Data Release 4 (Adelman-McCarthy et al. 2006) with a radius of $3.0''$. The PSF magnitudes of the u, g, r, i and z bands were adopted in this work. The near-infrared magnitudes were from the 2MASS point source catalog (Cutri et al. 2003), and default J, H and K_S band magnitudes were adopted.

2.3 Candidate Selection

Gorlova et al. (2004) studied the 24 μm emission of stars in M47, and found that the majority of them have a mean K_S–$[24]_{\rm Vega}$ value of 0.11 with a σ of 0.11 if described by a Gaussian distribution. Therefore they defined the 24 μm excess stars as those that were 3σ redder than the mean value, that is, K_S–$[24]_{\rm Vega} \geq 0.44$. We adopted their selection criterion to choose stars that show excess in 24 μm. $[24]_{\rm Vega} = [24]_{\rm AB} - 6.74$ was used to transform the AB magnitudes in the 24 μm band to the Vega magnitudes. To obtain the optical spectra, we only selected stars with r magnitudes less than 17.5. We also removed the objects with fuzzy features, whose 24 μm emission could come from the background galaxies. Finally, we selected eleven 24 μm excess candidates.

All the candidates' names and the optical to infrared magnitudes of the candidates are listed in Table 1. Since there are problems in the r magnitude of the star J163754.26+405259.1 and the g, r and i magnitudes of the star J163948.68+413711.0, we did not include these measurement in our subsequent analysis.

From Table 1 we can see that, except for J104508.69+592830.5, all these candidates have a K_S–$[24]_{\rm Vega}$ value above 1, indicating strong 24 μm excess. The optical r-band, IRAC 3.6 μm, 8.0 μm and MIPS 24 μm images are shown in Figure 1. The central circle in each image indicates the optical position of each star with a radius of $1.5''$. It can be seen that all the positions in the four bands are consistent.

Table 1 Names, magnitudes and colors of the eleven stars showing excess in 24 μm.

No.	Name	u	g	r	i	z	J	H	K_S	$[3.6]_{\rm AB}$	$[4.5]_{\rm AB}$	$[5.8]_{\rm AB}$	$[8.0]_{\rm AB}$	$[24]_{\rm AB}$	K_S–$[24]_{\rm Vega}$
1	J160551.07+534841.0	14.64	13.13	12.52	13.38	12.29	11.41	11.02	10.95	13.71	14.25	14.65	15.29	16.13	1.56
		±0.02	±0.00	±0.00	±0.00	±0.01	±0.02	±0.02	±0.02	±0.08	±0.08	±0.08	±0.08	±0.10	±0.10
2	J160650.59+543420.6	19.39	16.83	15.52	14.88	14.56	13.35	12.67	12.52	15.13	15.61	16.07	16.42	15.94	3.32
		±0.04	±0.02	±0.02	±0.02	±0.02	±0.03	±0.02	±0.02	±0.08	±0.08	±0.08	±0.08	±0.10	±0.10
3	J160122.04+545708.2	18.84	17.46	16.86	16.69	16.66	15.78	15.38	15.12	17.68	17.96	18.12	18.56	16.24	5.62
		±0.03	±0.03	±0.02	±0.02	±0.02	±0.07	±0.11	±0.13	±0.08	±0.08	±0.08	±0.09	±0.10	±0.17
4	J163754.26+405259.1	16.10	14.94	–	14.39	14.37	13.49	13.16	13.10	15.86	16.26	16.72	17.40	16.86	2.98
		±0.02	±0.01	–	±0.01	±0.02	±0.02	±0.03	±0.03	±0.08	±0.08	±0.08	±0.08	±0.10	±0.11
5	J163236.05+405537.3	16.34	15.28	14.85	14.76	14.77	13.82	13.54	13.43	16.13	16.58	16.96	16.39	16.41	3.76
		±0.02	±0.01	±0.01	±0.02	±0.02	±0.03	±0.05	±0.05	±0.08	±0.08	±0.08	±0.08	±0.10	±0.11
6	J163948.68+413711.0	14.85	–	–	–	13.25	12.44	12.19	12.18	14.90	15.35	15.88	16.51	17.01	1.91
		±0.01	–	–	–	±0.01	±0.02	±0.02	±0.02	±0.08	±0.08	±0.08	±0.08	±0.10	±0.11
7	J163611.64+412427.9	17.81	16.37	15.82	15.67	15.60	14.73	14.27	14.18	17.02	17.27	17.72	17.14	15.83	5.09
		±0.02	±0.02	±0.01	±0.02	±0.02	±0.03	±0.05	±0.06	±0.08	±0.08	±0.08	±0.08	±0.10	±0.12
8	J163730.40+403553.1	19.38	17.94	17.28	17.06	16.93	15.90	15.30	15.36	17.74	18.06	18.46	18.01	16.97	5.13
		±0.03	±0.01	±0.01	±0.01	±0.02	±0.08	±0.10	±0.19	±0.08	±0.08	±0.09	±0.08	±0.10	±0.22
9	J104508.69+592830.5	18.88	16.08	14.69	13.60	13.02	11.77	11.09	10.89	13.45	13.83	14.32	14.99	17.11	0.51
		±0.05	±0.01	±0.02	±0.02	±0.01	±0.03	±0.03	±0.02	±0.08	±0.08	±0.08	±0.08	±0.11	±0.11
10	J104205.94+594657.2	16.61	15.45	15.08	14.97	14.93	14.11	13.83	13.70	16.57	16.92	17.46	17.83	17.23	3.21
		±0.01	±0.03	±0.02	±0.01	±0.02	±0.03	±0.04	±0.04	±0.08	±0.08	±0.08	±0.08	±0.11	±0.12
11	J104537.18+570532.9	20.30	18.12	17.21	16.90	16.69	15.64	15.04	15.02	17.53	17.88	18.34	18.60	16.75	5.01
		±0.05	±0.02	±0.02	±0.02	±0.02	±0.07	±0.11	±0.14	±0.08	±0.08	±0.09	±0.09	±0.10	±0.18

Table 2 Log of observation, spectral type and fractional luminosity of the eleven stars showing excess in 24 μm.

No.	Name	Date of Obs.	Exptime (s)	Instrument	Slit (arcsec)	Sp.	$f_{\rm d}$
1	J160551.07+534841.0	Feb. 4, 2006	900	OMR 200 Å/mm	2.5	G8V	7.0E–5
2	J160650.59+543420.6	Apr. 28, 2006	2400	BFOSC Grism#4	1.8	M0V	7.4E–4
3	J160122.04+545708.2	May 6, 2006	3600	OMR 200 Å/mm	2.0	K0V	3.2E–3
4	J163754.26+405259.1	May 5, 2006	2700	OMR 200 Å/mm	2.0	G2V	2.1E–4
5	J163236.05+405537.3	Feb. 21, 2006	3600	BFOSC Grism#4	1.1	G3V	4.2E–4
6	J163948.68+413711.0	Feb. 4, 2006	1800	OMR 200 Å/mm	2.5	F8V	5.4E–5
7	J163611.64+412427.9	May 5, 2006	2700	OMR 200 Å/mm	2.0	G7V	1.8E–3
8	J163730.40+403553.1	May 6, 2006	3600	OMR 200 Å/mm	2.0	K4V	2.1E–3
9	J104508.69+592830.5	Feb. 3, 2006	2400	OMR 200 Å/mm	2.5	M3V	6.9E–5
10	J104205.94+594657.2	Feb. 3, 2006	2400	OMR 200 Å/mm	2.5	G0V	2.4E–4
11	J104537.18+570532.9	Feb. 3, 2006	3600	OMR 200 Å/mm	2.5	K6V	2.3E–3

2.4 Optical Spectroscopy

The optical spectra of 11 debris disk candidate stars were obtained with the 2.16 m telescope at Xinglong, NAOC (National Astronomical Observatories, Chinese Academy of Sciences) from February to May 2006. The spectrographs are either the OMR spectrograph with a dispersion of 200 Å/mm or BFOSC (Beijing Faint Object Spectrograph and Camera) with a G4 grism. Both spectrographs give a resolution of $\sim$ 10 Å and cover the wavelength range from 3800 Å to $\sim$ 8000 Å. The exposure times depend on the apparent magnitudes of these stars from 900 to 3600 seconds. Detailed

information of the spectral observations is presented in Table 2. All these spectral data were reduced by standard procedures with IRAF packages, including overscan correction for BFOSC only, bias subtraction and flat-field correction. He/Ne/Ar and Fe/Ar lamps were used for the wavelength calibrations of the OMR and BFOSC spectra, and KPNO standard stars were obtained to perform the flux calibration each night. All the resulting spectra are shown in Figure 2. The spectral classifications are given in Table 2. For those with poor signal-to-noise (S/N) in the spectrum (stars 3, 8 and

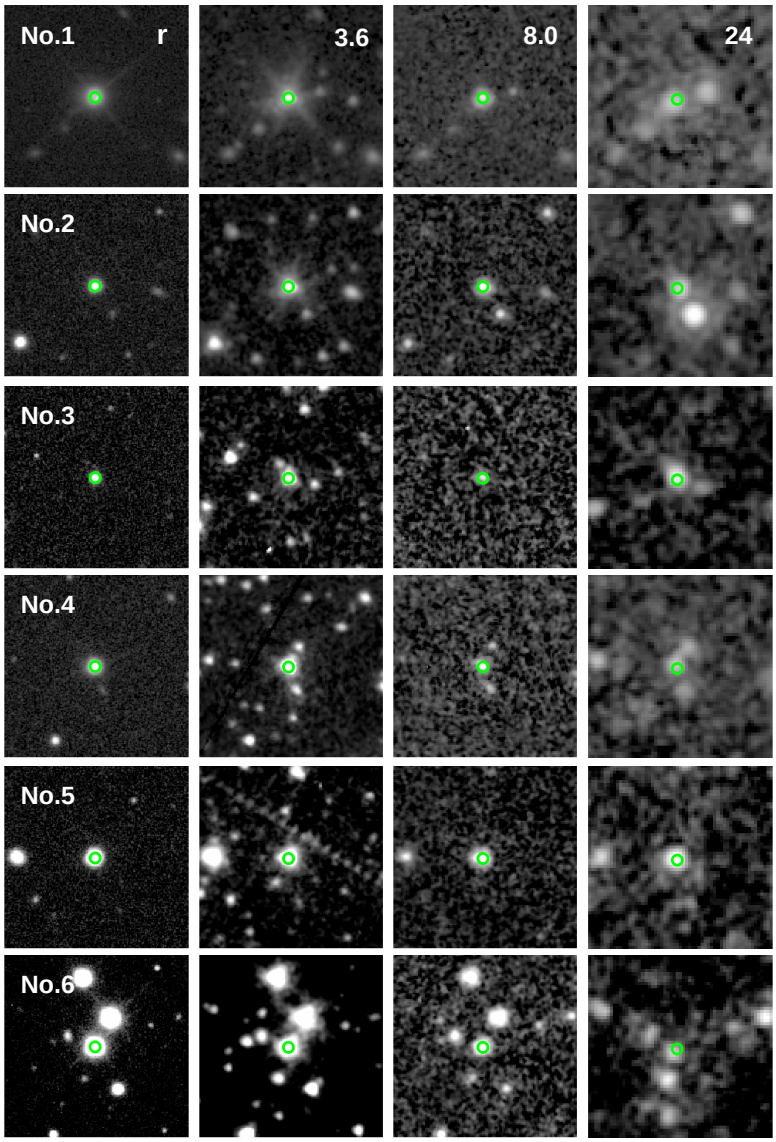

Fig. 1 Images of the SDSS r-band, and the Spitzer 3.6, 8.0 and 24 μm bands of the 24 μm excess stars. The circle in each image gives the position of the stars in the r-band with a radius of $1.5''$.

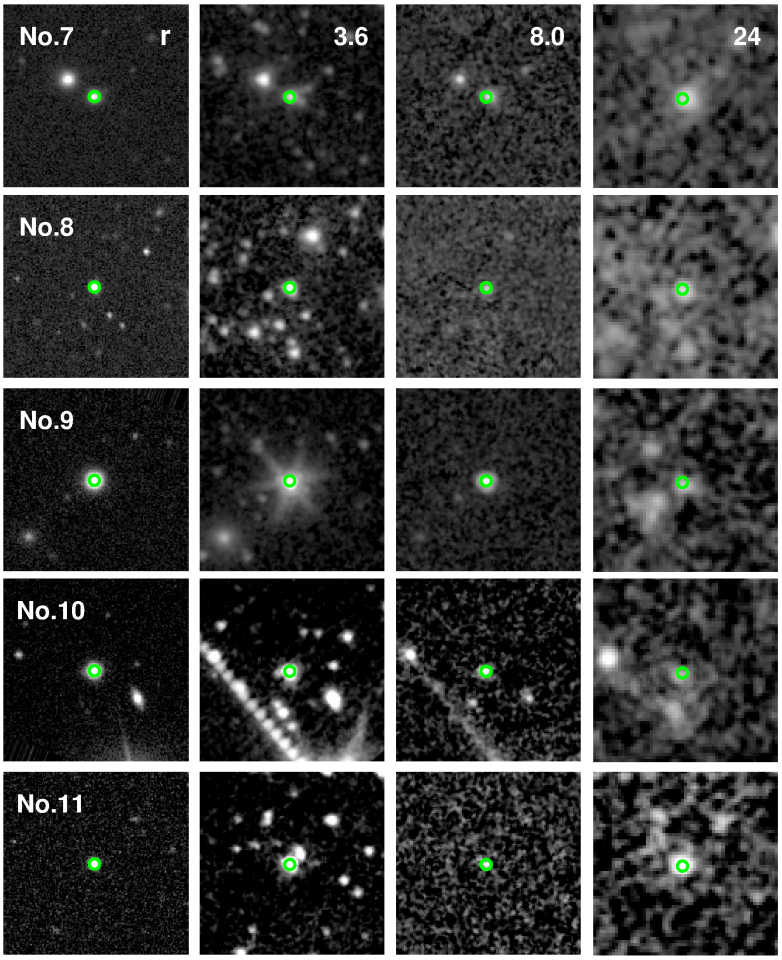

Fig. 1 —*Continued.*

11), we had to determine their spectral types according to their SEDs. All 11 stars are main-sequence dwarf stars, with spectral types from M to F, and are regarded as solar-like stars.

2.5 Reddening

Since all SWIRE regions are at high galactic latitudes, the extinction of all these stars by the Milky Way extinction A_V is no larger than 0.04 from the SDSS "star" catalog (Adelman-McCarthy et al. 2006) and is therefore neglected in the subsequent analysis. However, questions still remain about the local extinction of these stars.

Figure 3 shows the optical color-color diagram for nine stars. Due to the lack of some optical bands, stars J163948.68+413711.0 and J163754.26+405259.1 are not plotted in this figure. As a comparison, models of main-sequence stars and giants (Fitzgerald 1970) are also presented as different curves. All nine stars are consistent with late type stars as above and are located near the curve of the model stars. This indicates that all these stars are slightly obscured. The extinction of K_S is only 10% that of A_V and that of 24 μm is even smaller (Schlegel et al. 1998; McCall 2004; Rieke et al. 2005). Therefore all extinctions can be neglected.

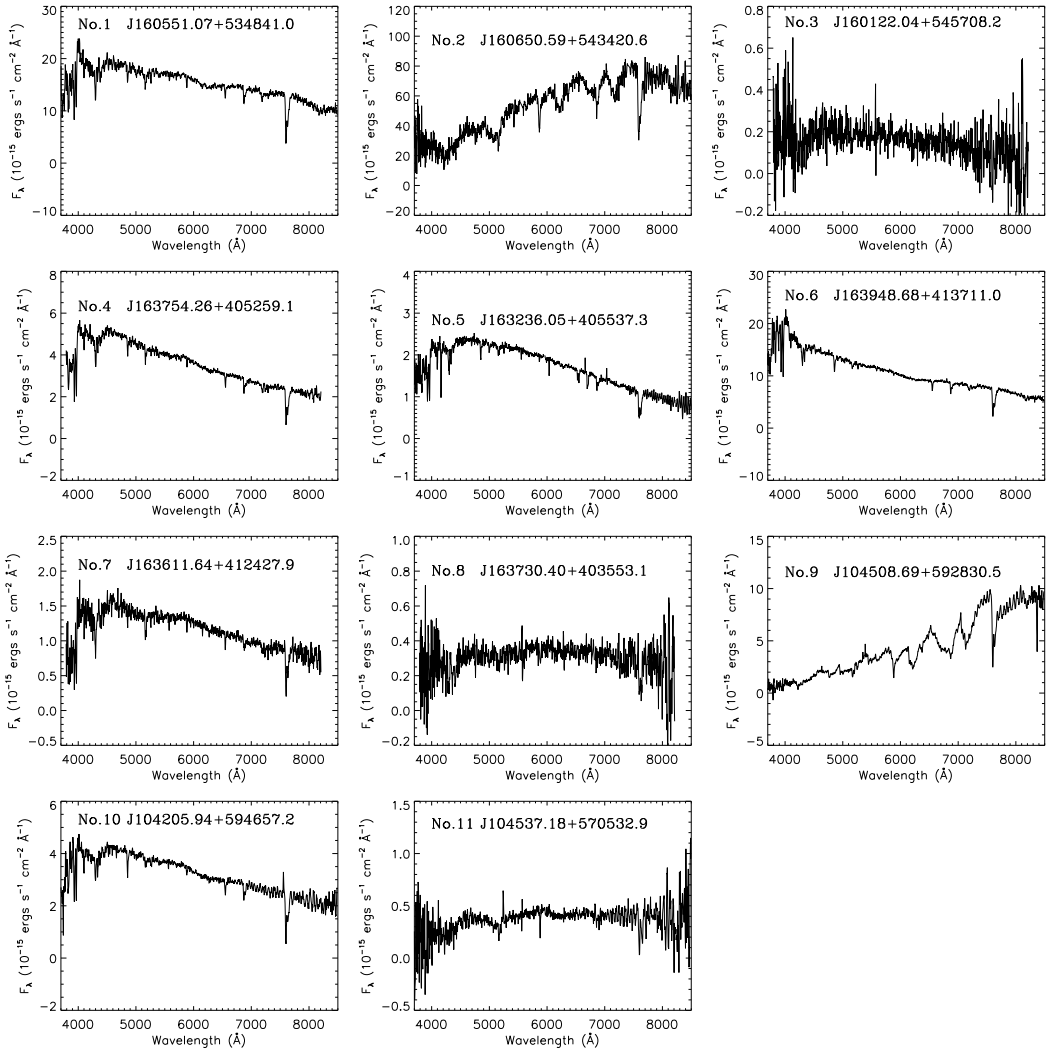

Fig. 2 Observed low-resolution optical spectra of the stars showing excess in 24 μm. Stars 3, 8 and 11 have very low S/N. All the stars present late-type star features.

3 RESULTS AND ANALYSIS

3.1 IRAC Colors

Figure 4 shows the mid-IR color-color plot for the 11 stars in the IRAC bands. The small circles represent the positions of the stars, and their corresponding numbers are also labeled. Vega is plotted as a star symbol. There are no obvious deviations in colors (either [3.6]–[4.5] or [3.6]–[8.0]) for stars 1, 4, 6 and 9 compared with Vega. Since Vega has proved to be a star with IR excess, for comparison we also plot the black-body position with a Vega temperature of 9600 K as a plus symbol. Both these stars and Vega show a minor excess from a black-body in the [8.0] band. However, stars 5, 7 and 8 show a large deviation (more than one magnitude) in the color range [3.6]–[8.0]. Such an 8 μm

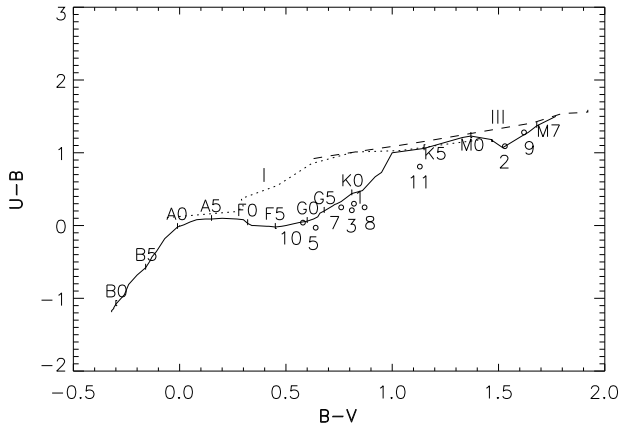

Fig. 3 Optical B–V versus U–B diagram of the stars showing excess in 24 μm. Each star is symbolized as a small circle and labeled with a number. Stars 4 and 6 are absent because of problems in some of the optical bands. The dotted line shows the normal dwarf stars in the color-color plot, and the corresponding spectral types are also labeled.

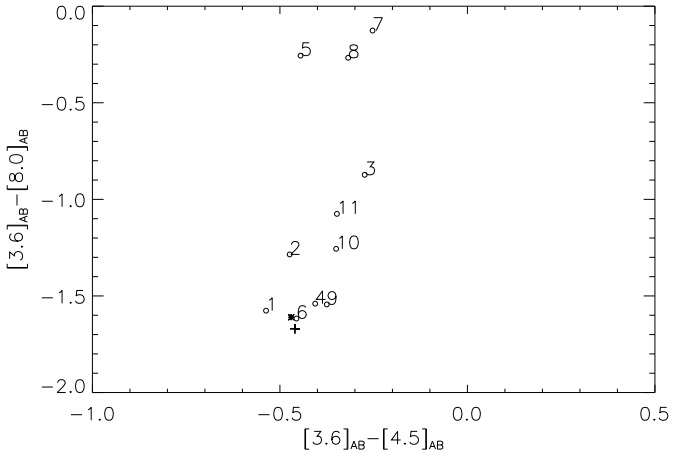

Fig. 4 Mid-infrared IRAC color-color diagram of the stars showing excess in 24 μm. All the colors are in the AB magnitude system. Each star is symbolized as a small circle and labeled with a number. The star and plus symbols represent the positions of Vega and a black-body with temperature of 9600 K. Three stars present a high mid-infrared excess at the 8 μm band, and four present a modest excess, with the other four showing a minor excess at the 8 μm band.

excess can be obviously seen in their SEDs in Figure 6. The remaining stars 2, 3, 10 and 11 show a marginal or modest deviation of [3.6]–[8.0], which represents a small excess at 8 μm in the SEDs (Fig. 6). Only two of these stars (stars 3 and 7) show a marginal deviation of [3.6]–[4.5], and the deviations are about 0.2, about 2–3 times the typical error. Therefore, we can be sure that most of these stars showing excess in 24 μm also show an excess in the 8 μm band, and in addition a few of them show an obvious excess in the 4.5 μm band.

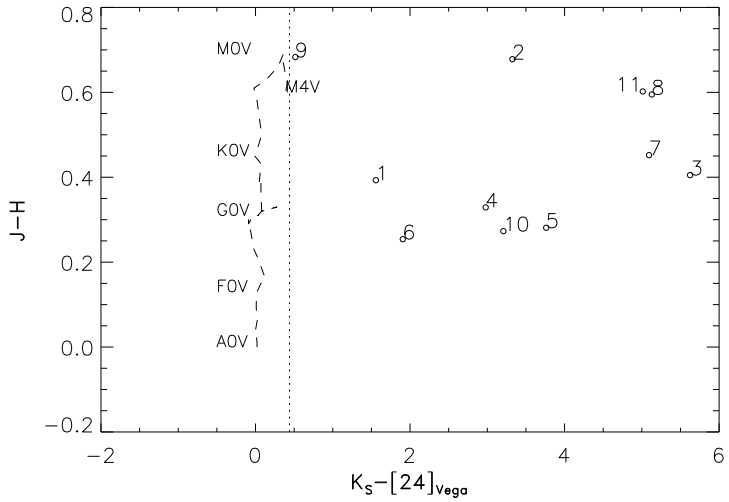

Fig. 5 Plot of J–H versus K_S–$[24]_{\rm Vega}$. All the colors are in the Vega magnitude system. Each star is symbolized as a small circle and labeled with a number. The dashed curve shows the normal dwarf stars labeled with the corresponding spectral types. The dotted line gives our criterion for selecting the 24 μm excess source. Apart from star 9, all stars have a K_S–$[24]_{\rm Vega}$ higher than a magnitude of 1, and four stars present a very strong excess in 24 μm.

3.2 MIPS 24 μm Excess and Fractional Luminosity

Figure 5 presents the J–H versus K_S–$[24]_{\rm Vega}$ diagram. The dashed line is the curve of main sequence stars and vertical dotted line is the selection criterion from Gorlova et al. (2004). All 11 stars are located in the upper late-type star region. This is consistent with the result of the spectral classification. Almost all of these stars present a large excess at 24 μm. Their K_S–$[24]_{\rm Vega}$ colors are larger than 1, and in some cases even up to 6. These values are far above our selection criterion value of 0.44. Only the late-type star 9 has a K_S–$[24]_{\rm Vega}$ value of 0.51, slightly larger than 0.44.

Unfortunately, we cannot obtain the confirmed far-infrared fluxes for all these stars because of the low resolution and low sensitivity of the *Spitzer* MIPS 70 μm and 160 μm bands. Without the total infrared luminosities of stars we cannot obtain the fractional luminosity $f_{\rm d}$, which is defined as the ratio of the integrated infrared excess of the disk to the bolometric luminosity of the star (Moór et al. 2006), to characterize the amount of dust. To roughly estimate the fractional dust luminosities, we assumed $F_{\rm IR} \sim \nu F_\nu[24\mu{\rm m}]$, as in Chen et al. (2005a). The bolometric luminosities of stars are from de Jager & Nieuwenhuijzen (1987), and the calculated fractional luminosities are listed in Table 2. The fractional luminosities range from 5×10^{-5} to 3×10^{-3}. It is quite interesting that four of these stars even have fractional luminosity values higher than 10^{-3}.

3.3 Spectral Energy Distributions

The SEDs of 11 stars are shown in Figure 6. They cover the wavelength range from the optical to the mid-IR bands, including the available photometries of SDSS u, g, r, i and z, 2MASS J, H and K_S, the four *Spitzer* IRAC bands and the MIPS 24 μm band. These stars exhibit a variety of mid-IR properties. Five of them only show an excess at 24 μm and four show obvious excesses at both 8 μm and 24 μm. Star 3 even presents an excess at a shorter wavelength of 3.6 μm. Apart from star 9, all

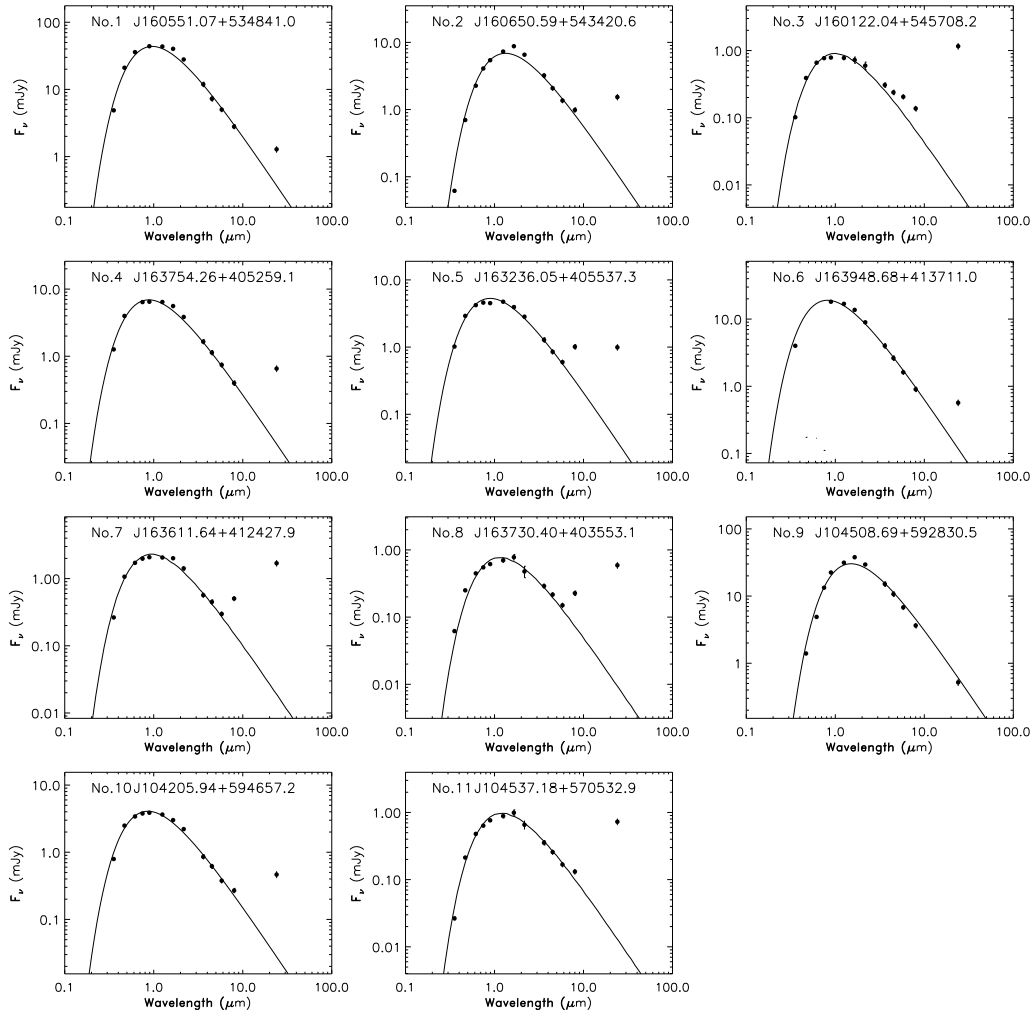

Fig. 6 Optical to mid-infrared SEDs of the 24 μm excess stars. The black points give the fluxes of the five SDSS bands (u, g, r, i, z), the three 2MASS bands (J, H, K_S), the four *Spitzer* IRAC bands and the MIPS 24 μm band. The photospheric emission is plotted as solid curves. When comparing with the solid curves, all these stars present an excess at the mid-infrared.

the stars show a deviation from the photosphere continuum at mid-IR, indicating the existence of an inner hole of the dust disk (Muzerolle et al. 2006; Young et al. 2004).

3.4 Notes For Individual Sources

J160551.07+534841.0, J160650.59+543420.6, J163754.26+405259.1, J163948.68+413711.0, J104205.94+594657.2: These stars have high S/N spectra and a moderate 24 μm excess (Fig. 5) with a K_S–$[24]_{\rm Vega}$ between 1 and 4. Their SEDs from the optical to IRAC bands are consistent with the photosphere continuum and only present infrared excess at 24 μm (Fig. 6).

J104508.69+592830.5: This is an M-type star from its spectra (Fig. 3). Though it satisfies the K_S–$[24]_{\rm Vega}$ criterion, it presents a marginal excess above the photospheric emission at 24 μm.

J163236.05+405537.3: This is a G-type star and the only source with an 8 μm flux higher than the 24 μm flux in the sample (Fig. 3 and Fig. 6). Such a feature indicates that the infrared emission peak is just between 8 μm and 24 μm, and the outer radius of the dust disk will be much smaller than 100 AU.

J104537.18+570532.9: Though it has low S/N in the spectra, when combined with its optical and near-infrared colors, we can still classify it as a K-type star. Its SED shows that there is little deviation from photospheric emission at 8 μm. However, it presents a high infrared excess at 24 μm (K_S–$[24]_{\rm Vega}\sim$5).

J163611.64+412427.9, J163730.40+403553.1: As above, with the low S/N spectra, J163730.40 +403553.1 was classified as a K-type star with the help of either the colors or the SED. J163611.64+412427.9 is a G-type star. Both stars show a high infrared excess at 24 μm. Their SEDs show an abrupt increase from 5.8 μm to 8 μm, and then an increase to 24 μm.

J160122.04+545708.2: For this source, we only have very low S/N spectra and classified it as a K-type star. With a K_S–$[24]_{\rm Vega}$ of 5.62, it is the strongest source showing an excess in 24 μm among the 11 stars. Its SED shows a deviation from photospheric emission even in the near-infrared band, indicating a smaller inner radius of the dust disk.

4 DISCUSSION

4.1 The Coincidence Probability

Though we excluded the sources with fuzzy features, it is still possible that some background and distant galaxies coincide with the position of the candidates and contribute to the measured radiation at 24 μm. Therefore, we need to estimate such a coincidence probability for each source. As in Stauffer et al. (2005), we first obtained the cumulative source counts for those with a 24 μm magnitude brighter than the star itself. Here we give an example to explain how we estimated the coincidence probability of star J160551.07+534841.0. Since it has a 24 μm magnitude of 16.1, we can estimate cumulative source counts of 7.8×10^5 per steradian for sources with a 24 μm magnitude less than 16.1 in the SWIRE ELAIS-N1 fields based on our catalog. This is consistent with that of the order of 7×10^5 per steradian for a flux density greater than 1.3 mJy (16.1 magnitude in the AB system) (Papovich et al. 2004) from another high galactic latitude field *Spitzer* xFLS. This corresponds to about one source per 54 000 arcsec^2, considering the previous matched radius of 3 arcsec. The coincidence probability of the background 24 μm source with a magnitude less than 16.1 being close to the line of sight to J160551.07+534841.0 is about 0.0005. Similarly, we estimated that the coincidence probabilities of the 11 stars are between 0.0003 and 0.003. Since all the stars are located at high galactic latitudes, it is impossible that it is contaminated by Galactic cirrus clouds. However, we still cannot exclude possible contamination by background AGNs (Stauffer et al. 2005).

4.2 Comparison with Other 24 μm Excess Samples

Until now, most of the detected 24 μm excess stars observed by *Spitzer* were young systems. Low et al. (2005) presented a 24 μm observation for 24 members of the 8–10 Myr old TW Hya association. They found four stars with a 24 μm excess. Young et al. (2004) detected several stars with a 24 μm excess from the young (25 Myr) cluster NGC 2547. Almost all of these stars have K_S–$[24]_{\rm Vega}$ colors less than 2. Only one shows a large K_S–$[24]_{\rm Vega}$ color up to 4. Gorlova et al. (2004) selected stars showing excess in 24 μm from the 100 Myr old open cluster M47. Seven of the early-type stars showed a smaller excess with K_S–$[24]_{\rm Vega}$=0.6–0.9 and one early type had a color value

of 2.4. Three late type stars had K_S–$[24]_{\rm Vega}$ colors between 1 and 4. By studying the 100 Myr old Pleiades cluster, Gorlova et al. (2006) obtained an excess fraction of 25% (5/20) for the early-type stars and 10% (4/40) for solar-type stars.

All of these stars had K_S–$[24]_{\rm Vega}$ colors less than 1.5. Chen et al. (2005a) obtained the observations of 40 F- and G-type members of the Scorpius-Centaurus OB association with ages between 5 and 20 Myr at 24 μm. They detected 14 objects that possessed 24 μm fluxes $\geq$ 30% larger than what would be predicted coming from their photosphere. Chen et al. (2005b) obtained the observations of 39 A- through M-type dwarfs with estimated ages between 12 and 600 Myr. Only three stars possessed a 24 μm excess. Su et al. (2006) reported the 24 μm measurements of 160 A-type main-sequence stars with ages ranging from 5 to 850 Myr. The 24 μm excess rate was 32%. Beichman et al. (2005) searched for debris disks showing infrared excess around 26 FGK field stars known to have one or more planets. All these stars had a median age of 4 Gyr. None of them showed an excess at 24 μm.

Including Beichman et al. (2005)'s sample, Bryden et al. (2006) extended the study to a well-defined sample of 69 FGK main-sequence field stars also with a median age of 4 Gyr. Only one star showed excess emission at 24 μm. Beichman et al. (2006) searched for the circumstellar dust around a sample of 88 F-M stars, and detected high S/N 24 μm emission in all cases, but only a few presented weak 24 μm excess, though 12 of them presented a significant excess of 70 μm emission. Morales et al. (2005) identified two new debris disk candidates with a 24 μm excess at high galactic latitude SWIRE fields.

Fajardo-Acosta et al. (2004) also searched for the 24 μm excess of main-sequence stars in another high latitude xFLS field. Koerner et al. (2010) presented 49 debris disk candidates that were within 25 pc of the Sun and with $V < 9$. The candidate 24 μm stars we found in the SWIRE fields are solar-like stars with possibly the oldest ages (see the following section). Most of them present a large 24 μm excess with K_S–$[24]_{\rm Vega}$, even approaching 6. Nowadays, only a few main-sequence stars have a comparably large 24 μm excess.

4.3 The Age

Though we have obtained the optical spectra of these 24 μm excess candidates and classified them based on their spectra and SEDs, we cannot determine their ages based on any of the five methods of age estimation for main-sequence stars (Lachaume et al. 1999). The low resolution of our spectra, and even poor S/N for some faint stars, prevented us from obtaining the ages by either rotation or iron abundance methods, which need high spectral resolution to measure the rotational velocities or fine absorption lines of different metal elements. The absence of calcium emissions and the large uncertainty of the distance determination of all these stars makes it impossible to obtain the ages based on calcium emission lines and isochrones. Since all these stars are field stars which are not born in molecular clouds, we cannot use the kinematics method either.

So what we can do is to determine their possible location (disk or halo) in our galaxy. As we now know, there are three components, excluding the bulge in our galaxy. They are the thin disk, the thick disk and the halo. The previous works (Bahcall & Soneira 1984; Gilmore 1984; Ojha et al. 1999; Chen et al. 2001; Du et al. 2003) showed that the scale heights of the thin disk were in the range 240 to 330 pc and the scale heights of the thick disk were in the range 580 to 1300 pc. Recently, Du et al. (2006) analyzed 21 BATC fields with 15 intermediate-band filters. The scale height they obtained for the thin disk varied from 220 to 320 pc and those for the thick disk varied from 600 to 1100 pc, which is consistent with previous results. Considering that all three SWIRE fields are at high galactic latitudes of about 40 to 50 degrees, more than half of the candidate stars have a vertical distance to the galactic plane above 600 pc (estimated from their spectral types), which is comparable to the scale height of the thick disk. Therefore, these stars could belong to the thick disk or even the halo.

The thick disk is an old component with an age of around 10 Gyr (Gilmore et al. 1995, 1989). It is quite possible that many of these candidates belong to the population of very old stars.

4.4 The Fractional Luminosity

There are two major zones of debris in the solar system: the asteroid belt at $2-4$ AU composed of rocky material that is ground up by collisions to produce most of the zodiacal dust cloud, and the Kuiper Belt that consists of small bodies orbiting beyond Neptune's orbit at 30–50 AU (Kim et al. 2005). The excess emission at the mid-IR bands *Spitzer* 24 μm and *IRAS* 25 μm are sensitive to material at several AU (Su et al. 2006). Therefore, the stars with a 24 μm excess are probably those with planetary systems containing a planetesimal belt corresponding to the asteroidal zone of the solar system (Gorlova et al. 2006). From a combination of observation and modeling, Backman & Paresce (1993) and Dermott et al. (2002) determined that the fractional luminosity of our asteroid belt is 10^{-8} to 10^{-7}.

Artymowicz (1996) argued that debris disks are confined to $f_{\rm d} < 10^{-2}$, and sources with higher fractional luminosity probably contain a significant amount of gas (e.g. T Tau and Herbig Ae/Be stars, other "transition" objects). Zuckerman & Song (2004) hypothesized that the stars with $f_{\rm d} > 10^{-3}$ are younger than 100 Myr, and therefore a high $f_{\rm d}$ value can also be used as an age indicator. This is supported by observations with ISO by Beichman et al. (2005), who suggested a decline in the fraction of stars with excess IR emission with time, but still having the possibility of modest ($f_{\rm d} > 10^{-5}$) excesses among the older stars (Decin et al. 2000, 2003). Meanwhile, Bryden et al. (2006) selected stars without regard to their age, metallicity, or any previous detection of IR excess. The stars have a median age of $\sim$4 Gyr. Their results show that debris disks with $f_{\rm d} \geq 10^{-3}$ are rare around old FGK stars.

On the contrary, Decin et al. (2003) claimed the existence of high $f_{\rm d}$ disks around older stars. Based on the general evolutionary trend described by Moór et al. (2006), the fractional luminosities of individual systems were found to show a large spread of $10^{-6} < f_{\rm d} < 10^{-3}$ at almost any age (Decin et al. 2003). Particularly interesting is the relatively high number of older systems ($t >$500 Myr) with high values of fractional luminosity ($f_{\rm d} \simeq 10^{-3}$).

Most of our candidates have values of fractional luminosity between 10^{-5} and 10^{-4}, and four of them even present high fractional luminosities greater than 10^{-3}. All four stars have a vertical distance to the disk above 900 pc and have a high possibility of being old solar-like stars in either the thick disk or the halo. Therefore, they are possibly the rarest systems found to date.

4.5 Physical Explanation and Challenges

How does such a large amount of dust still exist in very old solar-like stars? Due to the effect of radiation pressure, Poynting-Robertson drag and collisional destruction, the lifetime of the dust grains is quite short (Beichman et al. 2005; Rieke et al. 2005; Backman & Paresce 1993; Lagrange et al. 2000; Dominik & Decin 2003). For example, a dust grain with a smaller size ($\leq$ 1 μm) has a blow out time of less than 100 yrs, and a larger dust grain drifting from Poynting-Robertson drag would be destroyed on a timescale of 1–10 Myr (Kim et al. 2005). These are all far shorter than the age of the central stars. Therefore the dust observed must have been recently produced (Beichman et al. 2005). Rieke et al. (2005) pointed out that this recently produced dust in the "debris disk" would arise primarily from collisions between planetesimals and from cometary activity. However, the current model of gas planet formation and isotopic evidence from terrestrial and lunar samples indicate that Jupiter mass planets and Earth-Moon systems would have formed within several tens of millions of years (Silverstone et al. 2006; Kleine et al. 2002, 2003). This still cannot explain the phenomenon of high fractional luminosity in old stars. They raise a serious challenge even to the new generation of theoretical models (Moór et al. 2006). The most likely explanation for the presence

of debris disks with high fractional luminosity at ages well above a Gyr is the delayed onset of collisional cascades by late planet formation further away from the star (Dominik & Decin 2003). However, whether such a mechanism can also explain a very old star with an age of 10 Gyr is still questionable. Moreover, the most important aspect is to confirm the ages of these stars with high fractional luminosity, so spectra with higher S/N and higher resolution spectra are needed in future observations.

5 SUMMARY

We presented 11 debris disk candidates with distances from 300 to 2000 pc and ages of about 10 Gyr from *Spitzer* SWIRE fields, with the help of the SDSS star catalog and the 2MASS point source catalog. All the candidates presented an excess in 24 μm. The optical spectra obtained from the 2.16 telescope at Xinglong, NAOC and SEDs from the optical to mid-infrared are also presented. All these observations show the following.

All of the stars present late-type spectra and infrared fractional luminosities from 5×10^{-5} to 3×10^{-3}. They are solar-like stars with planetary debris disks. Except for J104508.69+592830.5, the SEDs of all the other stars indicate the existence of an inner hole in the dust disk.

We infer that many of these candidates would have ages of 10 Gyr, since they are located in the thick disk or in the halo of our galaxy. Therefore, four of these stars could belong to the oldest stars with high fractional luminosities ($f_{\rm d} \geq 1\times10^{-3}$). Though they have been quite rare until now, we indicate that high fractional luminosity debris disks can exist in old solar-like star systems.

With the release of the *Wide-field Infrared Survey Explorer* (WISE) data, progressively more candidates can be found (Wright et al. 2010). The discoveries of debris candidates at high galactic latitudes will provide an opportunity to study the properties and evolution of debris disk evolution in ISM poor environments.

Acknowledgements The authors would like to thank Jia-Sheng Huang, Zhong Wang, Jian-Rong Shi and Jing-Kun Zhao for useful discussions and advice on the *Spitzer* data reductions and spectral classification and the referee for their insightful comments. This project is supported by the National Natural Science Foundation of China (Grant Nos. 11173030, 11078017, 10833006, 10978014 and 10773014), and partly supported by the China Ministry of Science and Technology under the State Key Development Program for Basic Research (2007CB815400 and 2012CB821800). S. Wolf was supported by the German Research Foundation (DFG) through the Emmy Noether grant WO 857/2.

This work was supported by the Key Laboratory of Optical Astronomy, the National Astronomical Observatories, Chinese Academy of Sciences. This work was also, in part, based on observations made with the Spitzer Space Telescope, which is operated by the Jet Propulsion Laboratory of the California Institute of Technology under NASA Contract 1407. Funding for the SDSS and SDSS-II has been provided by the Alfred P. Sloan Foundation, the Participating Institutions, the National Science Foundation, the U. S. Department of Energy, the National Aeronautics and Space Administration, the Japanese Monbukagakusho, the Max Planck Society, and the Higher Education Funding Council for England.

The SDSS Web Site is *http://www.sdss.org/*. This publication makes use of data products from the Two Micron All Sky Survey, which is a joint project of the University of Massachusetts and the Infrared Processing and Analysis Center/California Institute of Technology, funded by the National Aeronautics and Space Administration and the National Science Foundation. *Facilities:* Spitzer, Sloan and the 2.16 m telescope (NAOC).

References

Adelman-McCarthy, J. K., Agüeros, M. A., Allam, S. S., et al. 2006, ApJS, 162, 38
Artymowicz, P. 1996, in The Role of Dust in the Formation of Stars, eds. H. U. Käufl, & R. Siebenmorgen (New York: Springer), 137
Aumann, H. H., Beichman, C. A., Gillett, F. C., et al. 1984, ApJ, 278, L23
Backman, D. E., & Paresce, F. 1993, in Protostars and Planets III, eds. E. H. Levy, & J. I. Lunine (Tucson: Univ. Arizona Press), 1253
Bahcall, J. N., & Soneira, R. M. 1984, ApJS, 55, 67
Beichman, C. A., Bryden, G., Rieke, G. H., et al. 2005, ApJ, 622, 1160
Beichman, C. A., Bryden, G., Stapelfeldt, K. R., et al. 2006, ApJ, 652, 1674
Benjamin, R. A., Churchwell, E., Babler, B. L., et al. 2003, PASP, 115, 953
Bertin, E., & Arnouts, S. 1996, A&AS, 117, 393
Brand, K., Brown, M. J. I., Dey, A., et al. 2006, ApJ, 641, 140
Bryden, G., Beichman, C. A., Trilling, D. E., et al. 2006, ApJ, 636, 1098
Bryden, G., Beichman, C. A., Carpenter, J. M., et al. 2009, ApJ, 705, 1226
Cao, C., & Wu, H. 2007, AJ, 133, 1710
Chen, A. B., Méndez, R. A., Tsay, W.-S., & Lu, P. K. 2001, AJ, 121, 309
Chen, C. H., Jura, M., Gordon, K. D., & Blaylock, M. 2005a, ApJ, 623, 493
Chen, C. H., Patten, B. M., Werner, M. W., et al. 2005b, ApJ, 634, 1372
Cutri, R. M., Skrutskie, M. F., van Dyk, S., et al. 2003, The IRSA 2MASS All-Sky Point Source Catalog, NASA/IPAC Infrared Science Archive. *http://irsa.ipac.caltech.edu/applications/Gator/*
de Jager, C., & Nieuwenhuijzen, H. 1987, A&A, 177, 217
Decin, G., Dominik, C., Malfait, K., Mayor, M., & Waelkens, C. 2000, A&A, 357, 533
Decin, G., Dominik, C., Waters, L. B. F. M., & Waelkens, C. 2003, ApJ, 598, 636
Dermott, S. F., Kehoe, T. J. J., Durda, D. D., Grogan, K., & Nesvorný, D. 2002, in Asteroids, Comets, and Meteors: ACM 2002 (ESA Special Publication), ed. B. Warmbein, 500, 319
Dominik, C., & Decin, G. 2003, ApJ, 598, 626
Du, C., Zhou, X., Ma, J., et al. 2003, A&A, 407, 541
Du, C., Ma, J., Wu, Z., & Zhou, X. 2006, MNRAS, 372, 1304
Evans, N. J., II, Allen, L. E., Blake, G. A., et al. 2003, PASP, 115, 965
Fadda, D., Marleau, F. R., Storrie-Lombardi, L. J., et al. 2006, AJ, 131, 2859
Fajardo-Acosta, S. B., Burgdorf, M. J., Cole, D. M., et al. 2004, in American Astronomical Society Meeting Abstracts #204, Bulletin of the American Astronomical Society 36, 773
Fazio, G. G., Hora, J. L., Allen, L. E., et al. 2004, ApJS, 154, 10
Fitzgerald, M. P. 1970, A&A, 4, 234
Gilmore, G. 1984, MNRAS, 207, 223
Gilmore, G., Wyse, R. F. G., & Kuijken, K. 1989, ARA&A, 27, 555
Gilmore, G., Wyse, R. F. G., & Jones, J. B. 1995, AJ, 109, 1095
Gorlova, N., Padgett, D. L., Rieke, G. H., et al. 2004, ApJS, 154, 448
Gorlova, N., Rieke, G. H., Muzerolle, J., et al. 2006, ApJ, 649, 1028
Habing, H. J., Dominik, C., Jourdain de Muizon, M., et al. 2001, A&A, 365, 545
Hollenbach, D. J., Yorke, H. W., & Johnstone, D. 2000, Protostars and Planets IV, 401
Houck, J. R., Soifer, B. T., Weedman, D., et al. 2005, ApJ, 622, L105
Hovhannisyan, L. R., Mickaelian, A. M., Weedman, D. W., et al. 2009, AJ, 138, 251
Huang, J.-S., Barmby, P., Fazio, G. G., et al. 2004, ApJS, 154, 44
Jannuzi, B. T., & Dey, A. 1999, in Astronomical Society of the Pacific Conference Series 191, Photometric Redshifts and the Detection of High Redshift Galaxies, eds. R. Weymann, L. Storrie-Lombardi, M. Sawicki,

& R. Brunner (San Francisco, CA:ASP), 111
Jourdain de Muizon, M., Laureijs, R. J., Dominik, C., et al. 1999, A&A, 350, 875
Kim, J. S., Hines, D. C., Backman, D. E., et al. 2005, ApJ, 632, 659
Kleine, T., Münker, C., Mezger, K., & Palme, H. 2002, Nature, 418, 952
Kleine, T., Mezger, K., & Münker, C. 2003, Meteoritics and Planetary Science Supplement, 38, 5212
Koerner, D. W., Kim, S., Trilling, D. E., et al. 2010, ApJ, 710, L26
Krist, J. E., Ardila, D. R., Golimowski, D. A., et al. 2005, AJ, 129, 1008
Lachaume, R., Dominik, C., Lanz, T., & Habing, H. J. 1999, A&A, 348, 897
Lacy, M., Wilson, G., Masci, F., et al. 2005, ApJS, 161, 41
Lagrange, A.-M., Backman, D. E., & Artymowicz, P. 2000, Protostars and Planets IV, 639
Lonsdale, C. J., Smith, H. E., Rowan-Robinson, M., et al. 2003, PASP, 115, 897
Low, F. J., Smith, P. S., Werner, M., et al. 2005, ApJ, 631, 1170
McCall, M. L. 2004, AJ, 128, 2144
Metchev, S. A., Hillenbrand, L. A., & Meyer, M. R. 2004, ApJ, 600, 435
Meyer, M. R., Hillenbrand, L. A., Backman, D. E., et al. 2004, ApJS, 154, 422
Moór, A., Ábrahám, P., Derekas, A., et al. 2006, ApJ, 644, 525
Morales, F. Y., Werner, M. W., Padgett, D., et al. 2005, in American Astronomical Society Meeting Abstracts, Bulletin of the American Astronomical Society 37, 1254
Muzerolle, J., Adame, L., D'Alessio, P., et al. 2006, ApJ, 643, 1003
Ojha, D. K., Bienaymé, O., Mohan, V., & Robin, A. C. 1999, A&A, 351, 945
Oke, J. B., & Gunn, J. E. 1983, ApJ, 266, 713
Papovich, C., Dole, H., Egami, E., et al. 2004, ApJS, 154, 70
Rieke, G. H., Young, E. T., Engelbracht, C. W., et al. 2004, ApJS, 154, 25
Rieke, G. H., Su, K. Y. L., Stansberry, J. A., et al. 2005, ApJ, 620, 1010
Schlegel, D. J., Finkbeiner, D. P., & Davis, M. 1998, ApJ, 500, 525
Silverstone, M. D., Meyer, M. R., Mamajek, E. E., et al. 2006, ApJ, 639, 1138
Spangler, C., Sargent, A. I., Silverstone, M. D., Becklin, E. E., & Zuckerman, B. 2001, ApJ, 555, 932
Stauffer, J. R., Rebull, L. M., Carpenter, J., et al. 2005, AJ, 130, 1834
Stoughton, C., Lupton, R. H., Bernardi, M., et al. 2002, AJ, 123, 485
Su, K. Y. L., Rieke, G. H., Stansberry, J. A., et al. 2005, LPI Contributions, 1280, 143
Su, K. Y. L., Rieke, G. H., Stansberry, J. A., et al. 2006, ApJ, 653, 675
Wen, X.-Q., Wu, H., Cao, C., & Xia, X.-Y. 2007, ChJAA (Chin. J. Astron. Astrophys.), 7, 187
Werner, M. W., Roellig, T. L., Low, F. J., et al. 2004, ApJS, 154, 1
Wright, E. L., Eisenhardt, P. R. M., Mainzer, A. K., et al. 2010, AJ, 140, 1868
Wu, H., Cao, C., Hao, C.-N., et al. 2005, ApJ, 632, L79
Wyatt, M. C., & Dent, W. R. F. 2002, MNRAS, 334, 589
Young, E. T., Lada, C. J., Teixeira, P., et al. 2004, ApJS, 154, 428
Zuckerman, B. 2001, ARA&A, 39, 549
Zuckerman, B., & Song, I. 2004, ARA&A, 42, 685